Neurobiology of Aging 74 (2019) 77–89

Contents lists available at ScienceDirect

Neurobiology of Aging

journal homepage: www.elsevier.com/locate/neuaging

Image-guided phenotyping of ovariectomized mice: altered functional connectivity, cognition, myelination, and dopaminergic functionality

Cynthia Anckaerts [a,*], Jaana van Gastel [b], Valerie Leysen [c], Rukun Hinz [a], Abdelkrim Azmi [b], Pascal Simoens [b], Disha Shah [a], Firat Kara [a], An Langbeen [d], Peter Bols [d], Charlotte Laloux [e], Vincent Prevot [c], Marleen Verhoye [a], Stuart Maudsley [b], Annemie Van der Linden [a]

[a] Bio-Imaging Lab, Department of Biomedical Sciences, University of Antwerp, Universiteitsplein 1, Wilrijk, Antwerp, Belgium
[b] Translational Neurobiology Group, Department of Biomedical Science, University of Antwerp-VIB, Universiteitsplein 1, Wilrijk, Antwerp, Belgium
[c] Development and Plasticity of the Neuroendocrine Brain, Inserm U1172, Jean-Pierre Aubert Research Centre, Labex Distalz, Lille cedex, France
[d] Veterinary Physiology and Biochemistry, Department of Veterinary Sciences, University of Antwerp, Universiteitsplein 1, Wilrijk, Antwerp, Belgium
[e] SFR DN2M, Inserm UMR-S1171/UMR-S1172, Lille cedex, France

ARTICLE INFO

Article history:
Received 5 June 2018
Received in revised form 20 September 2018
Accepted 6 October 2018
Available online 17 October 2018

Keywords:
Functional connectivity
Resting-state fMRI
Ovariectomy
Cognition
Behavior
Quantitative proteomics
Mass spectrometry
Myelination
Dopamine
Aging

ABSTRACT

A large proportion of the population suffers from endocrine disruption, e.g., menopausal women, which might result in accelerated aging and a higher risk for developing cognitive disorders. Therefore, it is crucial to fully understand the impact of such disruptions on the brain to identify potential therapeutic strategies. Here, we show using resting-state functional magnetic resonance imaging that ovariectomy and consequent hypothalamus-pituitary-gonadal disruption result in the selective dysconnectivity of 2 discrete brain regions in mice. This effect coincided with cognitive deficits and an underlying pathological molecular phenotype involving an imbalance of neurodevelopmental/neurodegenerative signaling. Furthermore, this quantitative mass spectrometry proteomics-based analysis of molecular signaling patterns further identified a strong involvement of altered dopaminergic functionality (e.g., DAT and predicted upstream regulators DRD3, NR4A2), reproductive signaling (e.g., Srd5a2), rotatin expression (rttn), cellular aging (e.g., Rxfp3, Git2), myelination, and axogenesis (e.g., Nefl, Mag). With this, we have provided an improved understanding of the impact of hypothalamus-pituitary-gonadal dysfunction and highlighted the potential of using a highly translational magnetic resonance imaging technique for monitoring these effects on the brain.

1. Introduction

Emerging research has demonstrated the involvement of the hypothalamus-pituitary-gonadal (HPG) axis in multiple nonreproductive processes, such as neurodevelopment, neuroplasticity, and various brain functions including cognition. Because the HPG system has a regulatory role on many organs, including the brain, age-related degeneration of this system also seems implicated in aging and pathophysiology of certain cognitive disorders, e.g., Alzheimer's disease (AD) (Koebele and Bimonte-Nelson, 2017; Wang et al., 2010; Zarate et al., 2017). In line with this, numerous studies have reported an association between HPG axis–related hormones (e.g., estrogen) and neurogenesis, neuroprotection, and cognition (for review, see Arevalo et al., 2015; Blair et al., 2015; Brann et al., 2007; Hara et al., 2015; Vargas et al., 2016). The trophic effect of sex steroid is critical in functions such as learning, memory, emotion, motivation, motor control, and cognition (Horstink et al., 2003; Sacher et al., 2013; Sakaki and Mather, 2012; Sundstrom Poromaa and Gingnell, 2014; Toffoletto et al., 2014). An important mechanism through which these actions can be exerted is via interaction with different neurotransmitter systems (for review, see Barth et al., 2015). The link between reproductive axis hormones and cognition is further highlighted by expression of both GnRH and estrogen receptors in brain regions important for memory and cognition (Albertson et al., 2008; Hazell et al., 2009; Mitra et al.,

* Corresponding author at: Bio-Imaging Lab, Department of Biomedical Sciences, University of Antwerp, Universiteitsplein 1, Wilrijk, Antwerp, Belgium. Tel.: +32 265 22 43.
E-mail address: Cynthia.anckaerts@uantwerpen.be (C. Anckaerts).

0197-4580/$ – see front matter © 2018 Elsevier Inc. All rights reserved.
https://doi.org/10.1016/j.neurobiolaging.2018.10.012

2003; Shughrue et al., 1997; Wen et al., 2011), such as hippocampal and cortical regions.

As menopausal women are prone to cognitive decline and have a higher risk of developing AD (Vina and Lloret, 2010), research has focused on the role of decreased estrogens (Li et al., 2014) or elevated gonadotropins, particularly luteinizing hormone (LH) (Blair et al., 2015, 2016), in these pathological events. Evidence suggests that such a lack of sex hormones can lead to aberrant neurotransmission, mitochondrial dysfunction, a decline of synaptic plasticity, brain hypometabolism and an increase of neuroinflammation (Zarate et al., 2017). Although a putative causal link between this hormonal system and both normal and pathological brain functionality is evidenced by many studies, clinical studies investigating the potential beneficial effect of modulating the HPG axis as a therapeutic target in menopausal women have failed to provide an unequivocal conclusion as to its potential utility (Henderson, 2014; Rocca et al., 2011). Therefore, it is crucial to obtain a better basic comprehension of the impact of HPG functionality on the brain as this knowledge could potentially be exploited to prevent the etiological development of cognitive disorders or help create new remedial drug strategies.

Ovariectomized (OVX) animals offer an experimental platform to study the impact of HPG dysfunction on the brain in a controlled manner (Koebele and Bimonte-Nelson, 2016). Surgical removal of ovaries, i.e., ovariectomy, will cause a sudden decrease of estrogen production hence disturbing the entire HPG system. More specifically, owing to the loss of negative feedback by estrogen, gonadotropin concentrations (LH; follicle stimulating hormone [FSH]) will increase, similar to the situation in natural or surgical menopause in women where loss of ovarian function has been linked to increased risk of various disorders such as Parkinson's disease or AD, depression, and anxiety (Parker et al., 2009; Rocca et al., 2008a,b, 2011, 2016, 2017). A disturbance of the balance within this hormonal system can lead to various effects in both human and rodents, including decreased neuroplasticity, loss of neuroprotective cellular signaling modalities, and neurotransmission deficits (Barth et al., 2015; Bosse and DiPaolo, 1996; Hara et al., 2015; Zarate et al., 2017). Furthermore, HPG dysfunction seems also linked to impaired cognitive function both in human and animal studies (Heikkinen et al., 2004; Iivonen et al., 2006; Toffoletto et al., 2014). However, interpreting this research is complicated because of the highly heterogeneous circumstances, e.g., differences in timing and duration of endocrine disruption as well as the type of potential hormone treatment. Despite some contradictory findings, the majority of current evidence points toward a significant effect of HPG-associated hormones on neural circuits implicated in cognition.

To examine neural circuits, resting-state functional magnetic resonance imaging (rsfMRI) has proven to be a valuable technique. This is a noninvasive in vivo tool capable of monitoring whole-brain functional connectivity (FC) based on the fact that low-frequency fluctuations (LFFs, 0.01–0.1 Hz) of the blood oxygenation level dependent (BOLD) contrast can be detected when a subject is at rest. This phenomenon of FC is defined as the temporal dependency of neuronal activation patterns of anatomically separated brain regions and can be calculated by correlating measures of the LFFs of the BOLD signal (van den Heuvel and Hulshoff Pol, 2010). It has been suggested that ovarian hormones could enhance both corticocortical FC and subcorticocortical FC, whereas androgens (testosterone) might decrease subcorticocortical FC but increase FC between subcortical brain areas (for review, see Peper et al., 2011). Only few human studies examined resting-state functional networks in (post)menopausal women or during the menstrual cycle showing either no changes (De Bondt et al., 2015; Hjelmervik et al., 2014) or FC alterations in brain regions such as the hippocampus and the frontal cortex (Comasco and Sundstrom-Poromaa, 2015; Huang et al., 2015; Lisofsky et al., 2015; Vega et al., 2016). Therefore, results concerning possible endocrine-driven functional alterations remain scarce and inconsistent. Going further on the idea that endocrine disruption could result in accelerated aging, long-range connections are of particular interest as it has been shown that these are most vulnerable to disintegrate during aging or disease processes (Dennis and Thompson, 2013; Fair et al., 2009; Tomasi and Volkow, 2012). For example, anterior-posterior (A-P) connectivity, i.e., the FC between anterior brain regions (frontal cortex) and posterior brain regions (posterior cingulate/retrosplenial cortex (RSC), medial temporal regions), has been shown to be high in young adults and to decrease during aging. Furthermore, the strength of this connection has been linked to cognitive performance as well (Andrews-Hanna et al., 2007; Vidal-Pineiro et al., 2014).

The present study was devised to examine whether a disturbance of the HPG axis can affect intrinsic functional brain networks in mice, reflecting an accelerated aging phenotype. For this purpose, mice were either ovariectomized or sham-operated at the onset of adulthood (age of 3 months). The intrinsic FC of the brain was monitored monthly using rsfMRI until the age of 7 months to evaluate whether altered patterns of FC could be identified after ovariectomy. Based on the rsfMRI outcome, complementary behavioral tests were performed in a separate cohort of 7-month-old mice to investigate whether FC deficits coincided with cognitive impairment. Finally, a quantitative mass spectrometry proteomics-based analysis of molecular signaling patterns was used to unravel the signaling mechanisms underlying the observed rsfMRI alterations in affected brain regions of 7-month-old OVX mice.

2. Material and methods

2.1. Ethical statement

All procedures were performed in strict accordance with the European Directive 2010/63/EU on the protection of animals used for scientific purposes. The research protocols used were approved by the Committee on Animal Care and Use at the University of Antwerp, Belgium (permit number 2014-56), and all efforts were made to minimize animal suffering.

2.2. Animals

C57BL/6J mice (12 weeks old, female, N = 36) were used throughout the MRI study (Jax mice strains, Charles River Laboratories). One week after a baseline rsfMRI scan at 3 months of age, i.e., the onset of adulthood, mice were randomly divided into 2 groups: an ovariectomized group (OVX, N = 18) and a sham-operated group (Sham, N = 18). After the surgical procedure, the diet was changed to a low-phytoestrogen diet (Sniff R/M-H, www.ssniff.de, Germany). Mice were assessed monthly using rsfMRI between the ages of 3 and 7 months. Owing to poor data quality (e.g., excessive movement or whole-brain unspecific FC), several scans were excluded, resulting in effective group sizes of 15–17 Sham mice and 13–18 OVX mice across the time points investigated (OVX: $N_{3M} = 13$, $N_{4M} = 18$, $N_{5M} = 16$, $N_{6M} = 16$, $N_{7M} = 14$; Sham: $N_{3M} = 16$, $N_{4M} = 16$, $N_{5M} = 17$, $N_{6M} = 16$, $N_{7M} = 15$). Behavioral analyses were performed in a separate cohort of 7-month-old mice ($N_{OVX} = 12$; $N_{Sham} = 11$) to avoid any confounding effect of repeated scanning/anesthesia on the behavioral outcome. From this group, brain tissue samples were collected for *ex vivo* analyses as described below. The selection of brain regions for further *ex vivo* analyses was guided by the rsfMRI readout.

2.3. Surgical procedure: ovariectomy

Before surgery, the weight of each animal was measured with a digital balance. Animals were anesthetized using an intraperitoneal injection of Anesketin (80–100 mg ketamine/kg BW)/Rompun (10 mg xylazine/kg BW)/Temgesic (0.1 mg buprenorphine/kg BW). Fur on the mouse abdomen was removed, and a small abdominal incision caudal of the umbilicus was made. After the peritoneal cavity was accessed, both left and right uterine tubes and ovaries were identified. Next, the distal part of both uterine horns, ovaries, and surrounding fat were removed by ligation using Vicryl suture 6-0 sutures for the OVX group. After removal of the ovaries, the abdominal cavity was closed (continuous sutures for the abdominal muscles; separate sutures for closing of the skin). The Sham group received a similar protocol where the abdominal cavity was accessed and then closed again, without removing any tissue or ligating any structures. After the surgical procedure, mice were allowed to recover in a heated cage and were observed until full recovery (Langbeen et al., 2016).

2.4. Plasma LH concentration

To ensure that the ovariectomy was successful in both cohorts of mice, the expected cessation of the estrus cycle was monitored by cytological examination of vaginal smears. Because OVX female mice showed constant estrus, plasma levels of the LH were measured in blood samples also collected in estrus in Sham mice, which were previously exposed to male urine via soiled bedding to synchronize their estrus cycles (Ryan and Schwartz, 1980; Whitten, 1956). LH was assayed using a protocol previously described by others (Messina et al., 2016; Steyn et al., 2013). A detailed description of the LH assay procedures can be found in Material and Methods (Supplementary Information).

2.5. Resting-state functional MRI procedure

For MRI procedures, mice were initially anesthetized with 2% isoflurane (IsoFlo; Abbott, Illinois, USA), which was administered in a mixture of 70% nitrogen (400 cc/min) and 30% oxygen (200 cc/min). During rsfMRI acquisitions, a combination of isoflurane (0.4%) and medetomidine (0.3 mg/kg; Domitor; Pfizer, Karlsruhe, Germany) was used to sedate the animals as previously described (Shah et al., 2016a,b). Briefly, mice received a subcutaneous bolus of medetomidine after which the isoflurane was reduced to 1%. Five minutes before the rsfMRI acquisition, isoflurane was further decreased to 0.4%. The rsfMRI acquisition was started 40 minutes after bolus injection while keeping the isoflurane level constant at 0.4%. After imaging procedures were performed, the effects of medetomidine were counteracted by the subcutaneous injection of 0.1 mg/kg atipamezole (Antisedan; Pfizer, Karlsruhe, Germany). The physiological status of the animals was monitored throughout the imaging procedure. A pressure-sensitive pad (MR-compatible Small Animal Monitoring and Gating System; SA Instruments, Inc.) was used to monitor breathing rate, and a rectal thermistor with feedback-controlled warm air circuitry (MR-compatible Small Animal Heating System; SA Instruments, Inc.) was used to maintain body temperature at 37.0 ± 0.5 °C.

MRI procedures were performed on a 9.4-T BioSpec MRI system (Bruker BioSpin, Germany) with Paravision 5.1 software. Images were acquired using a standard Bruker cross coil setup with a quadrature volume coil and a quadrature surface coil for the mouse brain. Three orthogonal multislice Turbo RARE T2-weighted images were acquired to render slice-positioning uniform (repetition time 2000 ms, echo time 15 ms, 16 slices of 0.4 mm). Field maps were acquired for each animal to assess field homogeneity, followed by local shimming, which corrects for the measured inhomogeneity in a rectangular volume of interest within the brain.

Resting-state signals were measured using a T2*-weighted single shot echo-planar-imaging sequence (repetition time 2000 ms, echo time 15 ms, 16 slices of 0.4 mm, slice gap 0.1 mm, 150 repetitions) with a total scan time of 5 minutes. The field of view was 20×20 mm^2 and the matrix size 128×64, resulting in pixel dimensions of 0.156×0.312 mm^2.

2.6. Resting-state data analysis

Preprocessing of the rsfMRI data was performed as described earlier (Jonckers et al., 2011). Realignment, normalization, and smoothing were performed using SPM12 software (Statistical Parametric Mapping, http://www.fil.ion.ucl.ac.uk). First, all images within each session were realigned to the first image. This was performed using a least-squares approach and a 6-parameter (rigid body) spatial transformation. Second, all data sets were normalized to a study specific echo-planar-imaging template obtained by averaging all baseline scans. The normalization steps consist of a global 12-parameter affine transformation followed by the estimation of the nonlinear deformations. Finally, plane smoothing was performed using a Gaussian kernel with full width at half maximum of twice the voxel 0.31×0.62 mm^2 (Jonckers et al., 2011). Next, resting-state data were filtered (0.01–0.1 Hz) using the Resting-State fMRI Data Analysis Toolkit (REST1.8) in Matlab 2014a to extract relevant data and rule out noise and low-frequency drift. Owing to poor quality or excessive movement, several scans had to be excluded, resulting in effective group sizes of 15–17 Sham mice and 13-18 OVX mice across the time points investigated.

Independent component analysis (ICA) was performed on the rsfMRI data of 3-month-old animals, to determine which resting-state networks could be observed in healthy animals (Jonckers et al., 2011). ICA was performed using the GIFT-toolbox (Group ICA of fMRI toolbox version 2.0a: http://icatb.sourceforge.net/), by implementing spatial ICA, which estimates sources as being statistically spatially independent. First, a two-step data reduction step is performed by principal component analysis, after which the data of each individual animal are concatenated. Then, group ICA was performed using the Infomax algorithm. The final step is back reconstruction of the data to single-subject independent components and time courses. ICA was performed using a preset of 15 components, which was shown to be appropriate to identify relevant resting-state networks in mice. Based on this analysis, the anterior/prefrontal and posterior/retrosplenial FC networks were identified, and masks were created from the relevant ICA components.

Regions of 4 voxels each were indicated with the anatomically relevant ICA components and the Mouse Brain Atlas (Franklin, 2007) as reference in MRIcron software (http://www.mricro.com/mricron). For the anterior/prefrontal network, the following seeds were indicated: left and right anterior cingulate cortex (aCg) and prelimbic cortex (PrL). For the posterior/retrosplenial network, seeds were selected in the left and right RSC and parietal association cortex (PaA). These seeds were then used to extract the respective temporal signal of each subject using Rest 1.8.

Anterior-posterior (A-P) connectivity was calculated in 2 different ways: (1) based on a region of interest (ROI)–based analysis or (2) based on a seed-based analysis. Method (1) involved the computation of all pairwise correlations (z-values) between the rsfMRI time series of regions of the anterior network (aCg, PrL) and the posterior network (RSC, PaA) resulting in a functional connectivity (zFC) matrix. More specifically, for ROI-based FC analysis, the BOLD time course of each seed region was extracted after which linear correlation between the selected time courses, i.e., a measure

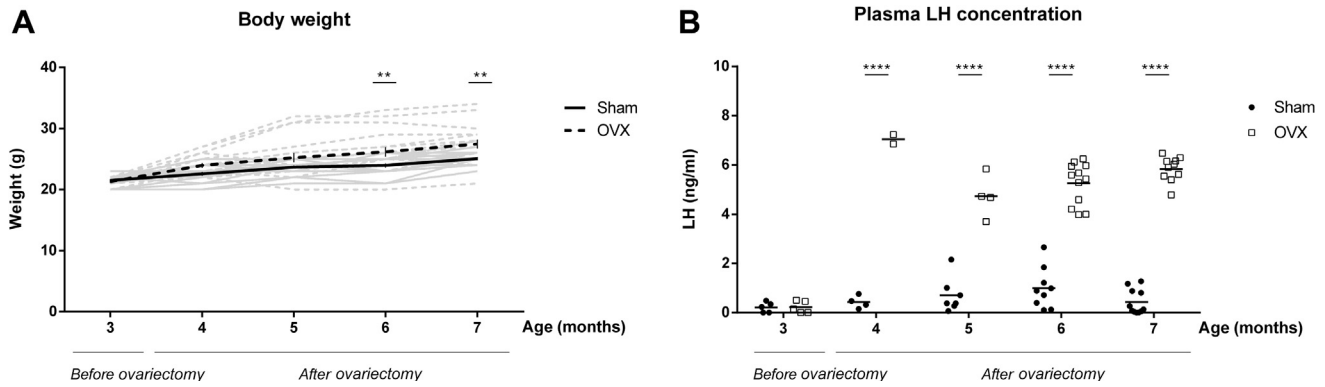

Fig. 1. Body weight (A) and plasma luteinizing hormone (LH) concentration (B). (A) Illustration of weight gain for both ovariectomized (OVX) and Sham groups over time. OVX mice had higher body weights than sham mice at 6 and 7 months of age. Results shown as mean ± SEM; individual values are indicated in light gray lines. (B) Plasma LH concentration for both groups over time showing elevated plasma LH after ovariectomy. ** $p < 0.01$; **** $p < 0.0001$. Results are shown as mean overlaid on the individual values.

of the strength of FC between the respective ROIs, was calculated using a cross-correlation analysis in REST 1.8. A Fisher's z transform was performed on all correlation coefficients. The z-transformed correlation values were presented in a zFC matrix, with a threshold to exclude z-values below 0.05 ($|z| < 0.05$) (Shah et al., 2016c). Next, these individual pairwise FC values were classified according to the anterior or posterior network and were used for further between-network FC computations, i.e., the average of all pairwise correlations between anterior and posterior regions. Method (2), based on a seed-based analysis of the Rs cortex, involved the computation of individual statistical FC maps. Briefly, the extracted temporal signal of the Rs seed was compared to all other voxels of the brain using a linear model in SPM12, resulting in individual FC maps containing all voxels significantly correlated with the given temporal signal. Next, individual t-values were extracted for each subject within the restrictions of the anterior network (ICA component) mask. In addition, individual cluster sizes were extracted from the subject's statistical FC maps within the restrictions of the relevant ICA component masks.

2.7. Behavioral assessments

To evaluate whether FC changes as observed by rsfMRI at the age of 7 months coincided with behavioral deficits, a separate cohort of 7-month-old Sham and OVX mice was subjected to a series of behavioral tests. Similar to the first cohort, these mice were ovariectomized or sham-operated 4 months before testing, i.e., at the age of 3 months. Behavioral tests were specifically selected based on the regions affected according to the rsfMRI outcome and included the spontaneous alternation (SA) test, novel object recognition (NOR) test, Barnes maze, and passive avoidance (PA) test.

2.7.1. Y-maze SA test

The SA test (Hughes, 2004) was used to assess working memory of mice in a Y-maze (3 arms of 8 × 30 cm), which requires proper function of hippocampal and frontal brain regions (Lalonde, 2002). Furthermore, it has been shown that working memory can be modulated by aging and hormonal status (Cao et al., 2013; Lalonde, 2002). This test is based on the fact that mice will show the tendency to explore the different arms with alternation of arms visits rather than returning to the previous arm. Mice were placed in one of the arm (randomized between subjects) and allowed to explore the entire maze for 8 minutes. Every entry to an arm was recorded and defined as entering the arm with all 4 paws. Performance of mice in this test was calculated as percentage alternation, defined as the ratio of the number of triads (entering each of the 3 arms consecutively) over the total number of arm entries.

2.7.2. NOR test

The NOR test was used to assess recognition memory, involving frontal and parietal association cortices (Leger et al., 2013). Interestingly, Fonseca et al. and Bastos et al. previously reported impairments in NOR after ovariectomy, which could be recovered by hormone replacement therapy (Bastos et al., 2015; Fonseca et al., 2013). The NOR consisted of an initial habituation day in which the mice were placed in an empty arena (50 × 50 cm) for 10 minutes to acclimatize to the novel environment. The following day, 2 identical objects (pair A) were placed on opposite sides in the cage. During the object exploration training, the mouse was placed in the arena and was allowed to explore the objects for 15 minutes. On the test day, 24 hours later, the animals were placed in the arena for 15 minutes, which contained two identical objects (pair B, different than the previous day). One hour later, the mouse was again placed into the arena for 5 minutes, which now contained one familiar object (of pair B) and one completely new object. To assess the recognition memory function, the discrimination index was calculated as the ratio of the time spent exploring the new object over the total objects exploration time.

2.7.3. Barnes maze

The Barnes maze was used for measuring visuospatial learning and memory (Sunyer et al., 2007). By altering the specific setup of this test, both learning and long-term memory can be evaluated. Spatial memory is dependent on various brain regions, including the hippocampus, parietal cortex, entorhinal cortex, prefrontal (Pf) cortex, and retrosplenial (Rs) cortex. Importantly, the learning phase of this test is highly dependent on hippocampal function, whereas the later memory retention phase strongly relies on cortical integration (Bontempi et al., 1999; Izquierdo and Medina, 1997; Maviel et al., 2004; Miller, 2000; Todd and Bucci, 2015). Alterations in spatial memory and retention have been reported previously after hormonal modulations (Ping et al., 2008; Sandstrom and Williams, 2001; Sarkaki et al., 2008).

The Barnes maze consisted of a circular platform (120 cm of diameter) with 40 equally spaced holes, of which one target hole gave entrance to a dark target box. The maze was surrounded by visual cues of different colors and shapes. The test consisted of an initial 4 training days and 1 test day (day 5). For each trial, the animal was placed onto the middle of the maze in an opaque cylindrical tube to ensure an initial disorientation before starting. Each trial is initiated by removing the opaque cylinder. On the first

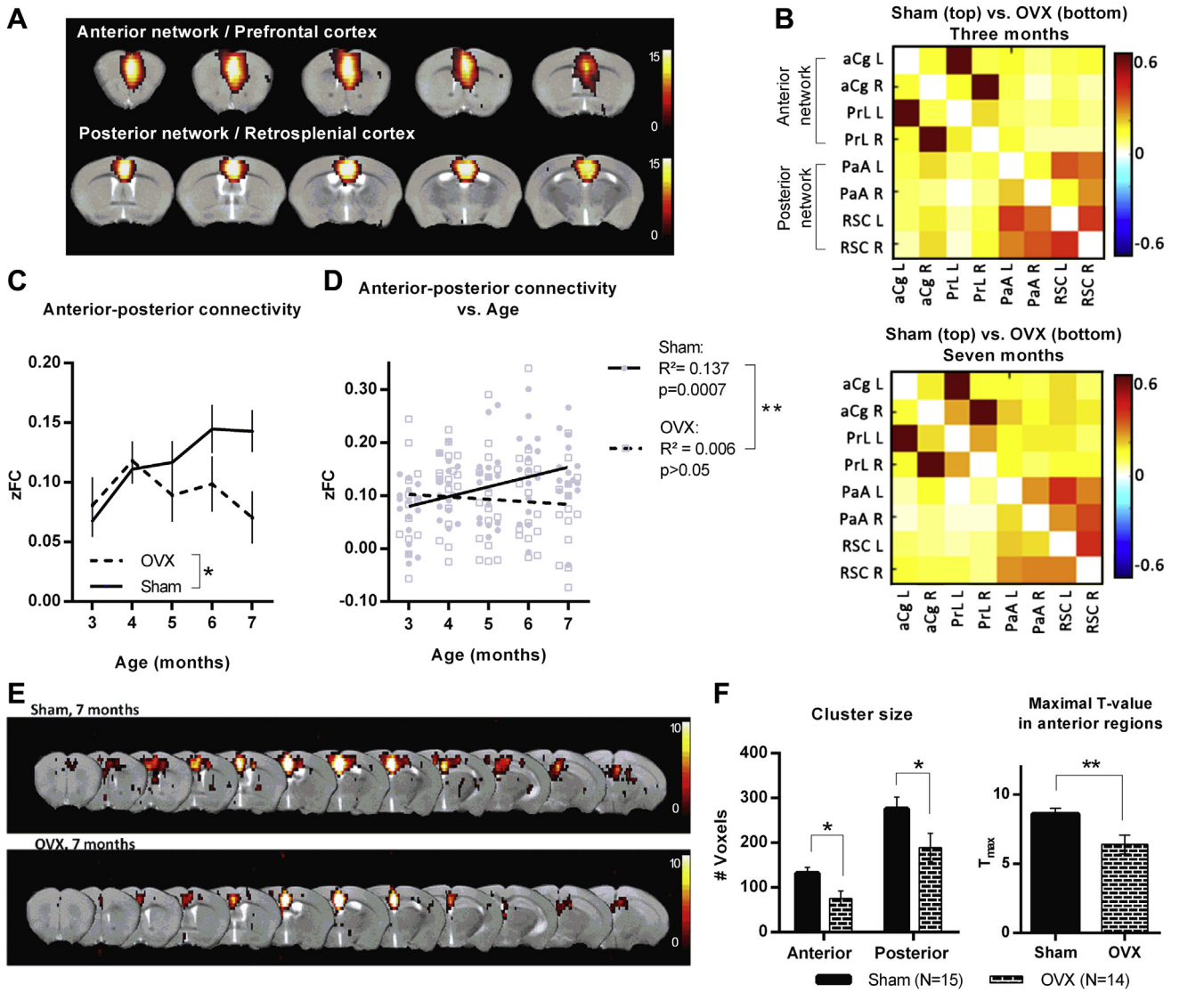

Fig. 2. Aberrant A-P FC in ovariectomized mice. (A) Illustration of relevant ICA components obtained from the group-level ICA of baseline rsfMRI data. The color scale represents t-values with yellow indicating a stronger correlation. (B) Average zFC matrices for 3- and 7-month-old Sham and OVX mice. Each square represents the correlation between a pair of ROIs with the color scale representing z-values. (C) FC between the anterior and posterior networks, based on matrices as illustrated in (B). OVX mice have consistently lower A-P FC than Sham mice. (D) Average A-P FC in 2 distinct age categories. Sham mice have significantly higher A-P FC at adult ages than OVX mice. (D) Linear regression analysis between A-P FC and age showing a significant positive correlation in the Sham group only. (E) Group-averaged statistical FC maps obtained from a seed-based analysis at 7 months with the RSC as seed. Results are shown uncorrected, $p < 0.001$, cluster size $k > 10$, overlaid on an anatomical T2-weighted image. The color scale indicates t-values with yellow representing a higher correlation with the seed region. (F) Cluster size (left graph) within the restrictions of the anterior and posterior network masks (A) for a seed in the RSC (E). Maximal t-values (right graph) within the anterior network for a seed in the RSC (E) confirm reduced A-P FC in OVX mice at 7 months. * $p < 0.05$; ** $p < 0.01$. Results are shown as mean ± SEM. Abbreviations: aCg, anterior cingulate cortex; A-P FC, anterior-posterior functional connectivity; ICA, independent component analysis; PrL, prelimbic cortex; PaA, parietal association cortex; RSC, retrosplenial cortex; rsfMRI, resting-state functional magnetic resonance imaging; L, left; R, Right; OVX, ovariectomized. (For interpretation of the references to color in this figure legend, the reader is referred to the Web version of this article.)

day, the mouse was allowed to explore and guided to its respective escape hole and left inside for 1 minute. Next, the training consisted of 4 days with 4 trials of 3 minutes per mouse (15 minutes in between every trial). The same target hole was used for one subject along all the training, with a different target hole between subjects. On day 5, the first test day, no escape box was placed and the animal was allowed to explore the platform for 90 seconds. This final test was repeated 1 and 2 weeks after training, on day 12 and 19, respectively, to assess the long-term retention ability of mice (Sunyer et al., 2007). Primary errors were assessed by counting the number of wrong escape holes a subject explored before finding the correct target hole. Primary latency was calculated, i.e., the time it took for a subject to find the target hole. In case a subject was not successful, this time was set at 90 seconds as a cutoff time. Finally, the time spent in the target area was assessed as subjects should show a preference for this area of the maze.

2.7.4. PA test

The PA test was used to evaluate aversive learning, which involves various brain regions such as the Pf and amygdala. Especially, the cholinergic system has been linked to performance in this test, and impaired performance has further been observed after ovariectomy (Das et al., 2002). Passive avoidance learning was tested in a step-through box (Marciniak et al., 2015). The step-through box consisted of an aversive brightly lit compartment connected with a dark compartment by means of a sliding door. Mice were placed in

the illuminated compartment during 90 seconds at maximum, and after 5 seconds, the sliding door connecting both compartments was opened. Upon complete entry into the dark compartment (4-paw criterion), animals received a slight foot shock (0.2 mA, 2 seconds). Exactly 24 hours later, mice are placed once again in the illuminated compartment and the escape latency to re-enter the dark compartment was timed up to 300 seconds.

2.8. Mass spectrometry and quantitative proteomics of murine cortex samples

To elucidate the molecular signaling pathways responsible for the OVX-induced alterations of FC and cognition, an unbiased quantitative proteomic approach using iTRAQ (isobaric mass-tag labeling for relative and absolute quantitation) mass spectrometry was applied to simultaneously identify and quantify the proteins that are differentially upregulated or downregulated in fresh frozen murine cortical samples of OVX or Sham mice. Based on the outcome of the rsfMRI analysis, Pf and Rs cortices samples were collected from mice previously subjected to the behavioral assessments (average age: 7.7 months; $N_{Sham} = 4$; $N_{OVX} = 4$) and processed as described in detail in Material and Methods (Supplementary Information).

Briefly, the raw data were analyzed by Proteome Discoverer 2.0 Software (Thermo Scientific) using Sequest HT as search engine against the human UniProt/SwissProt database with threshold of confidence above 99% (false discovery rate < 1%). The list of identified proteins, containing iTRAQ ratios of expression levels over control (Sham) samples, was generated. Proteins identified according to the statistical MS cutoffs were then subsequently used for further bioinformatics analyses. To identify the significantly altered proteins, i.e., proteins differentially expressed due to ovariectomy surgical intervention exposure compared to sham surgery exposure, raw iTRAQ ratios (OVX:Sham) were first $\log_2$ transformed. Following $\log_2$ ratio transformation, differentially expressed protein (DEP) lists were created by identifying only proteins that possessed $\log_2$-transformed iTRAQ ratios two standard deviations ($p < 0.05$) from the calculated mean background expression variation level. These results were further verified with Western blots.

Significant DEP lists (comprising proteins elevated or reduced in their expression in cortex tissue samples in response to OVX surgical intervention) were then employed for further bioinformatics deconvolution using diverse informatics platforms including Ingenuity Pathway Analysis (IPA) (Canonical Signaling Pathway and Upstream Regulator applications; https://www.qiagenbioinformatics.com/products/ingenuity-pathway-analysis/), VennPlex (Cai et al., 2013; https://www.irp.nia.nih.gov/bioinformatics/vennplex.html), and Network Analyst (http://www.networkanalyst.ca/).

Finally, a targeted natural language processing (NLP) investigation was performed to identify the specific functional intersection between steroid-related activity (implementation of ovariectomy) and the DEP data sets from both cortical samples. To this end, using the latent semantic indexing platform GeneIndexer, the specific DEPs from either data set could be associated with our user-defined concept terms related to estrogenic activity in the brain. GeneIndexer is able to identify the strongest concept (user-defined input word) and term (Gene Symbol) correlation scores for any given input data set using gene-word document analysis of over 20 million curated PubMed abstracts (Cashion et al., 2013; Chen et al., 2013). Here, we used the word concepts *menopause, aging, ovariectomy, estrogen/oestrogen, estradiol/oestradiol*, and *estrogen receptor/oestrogen receptor* to identify the most strongly associated proteins across all of these terms from both Pf and Rs cortex DEP data sets. To simplify the numerical analysis of this output, the following synonymous term cosine similarity scores were summed together to create a comprehensive score, i.e., scores for "*estrogen*," "*oestrogen*," "*estradiol*," and "*oestradiol*" were summed together, and scores for "*estrogen receptor*" and "*oestrogen receptor*" were also summed.

Through ranking of the top 20 strongest correlating proteins (via both sum and mean of the cosine similarity scores across all the input concepts), a prioritized key group of proteins for each DEP list was created. Using *Enrichr*-based (http://amp.pharm.mssm.edu/Enrichr/) interrogation of ligand-induced Gene Expression Omnibus (GEO) data set alterations (https://www.ncbi.nlm.nih.gov/geo/), lists of strongly correlating ligand-controlled curated GEO response data sets were generated for the Rs and Pf cortex input data sets (20 proteins). We next extracted the specific words describing the significantly associated ($p < 0.05$) ligand-controlled GEO data sets and then created frequency-dependent wordclouds from these ligand terms. Next, these proteins were cross-interrogated with a functional disease database (also via Enrichr), i.e., the JENSEN Disease database (https://diseases.jensenlab.org/) to identify possible related disorders.

2.9. Statistical analyses

Statistical analyses of the physiological parameters, FC data, and the behavioral data were performed in Graphpad Prism 6.0 using a linear mixed model analysis in JMP Pro 13 software with group and age as fixed effects and subject as random effect. In case no significant interaction effect [age × group] was found, only main effects (group or age) are reported. *Post hoc* tests were performed using the Tukey HSD (honest significance difference) multiple comparison test with $p < 0.05$. To explore the A-P FC pattern in both groups in more detail, an additional hypothesis-driven analysis of group-specific aging effects was performed by performing a mixed model analysis split by group (i.e., explore the age effect within each group separately). Finally, to evaluate the relation between age and A-P FC strength, a linear regression analysis was performed. To evaluate whether the outcome of this linear regression differed significantly between both groups, a one-way analysis of covariance was performed to evaluate the effect of age on A-P FC with group (OVX or Sham) as covariate.

Group-wise average seed-based FC maps were computed in SPM12 software using a one-sample *t*-test (uncorrected $p < 0.001$; minimum cluster size $k > 10$; Shah et al., 2018). The extracted t-values as well as cluster sizes were examined using two-sample t-tests. In case of multiple t-tests in parallel, a Holm-Sidak correction for multiple comparisons was applied ($p < 0.05$).

Results obtained from the Western blots were examined using unpaired t-tests to evaluate whether expression of the specific proteins differed significantly between OVX and Sham mice.

All reported values are shown as mean ± standard error.

3. Results

3.1. Increased body weight and plasma LH after ovariectomy

An analysis of body weight and plasma LH of OVX and Sham mice revealed a significant [age × group] interaction effect ($F_{4,136} = 6.478$, $p < 0.0001$; Fig. 1A). Although both groups gained a significant amount of weight during the experiment, a clear distinction was present between both groups. As such, the OVX group ranged from 21.28 ± 0.18 g at 3 months to 27.44 ± 0.72 g at 7 months, whereas the Sham group only ranged from 21.5 ± 0.22 g at 3 months to 25.06 ± 0.26 g at 7 months. According to the *post hoc* analysis, only the OVX group gained a significant amount of body weight 1 month after the surgery, i.e., at 4 months of age (3M vs. 4M: $p_{OVX} < 0.0001$; $p_{Sham} = 0.2303$). In contrast, Sham mice gained

weight at a slower rate than the OVX group (3M vs. 5M: $p_{OVX} < 0.0001$; $p_{Sham} < 0.0001$). This difference in body weight between both groups became significantly different starting at the age of 6 months, i.e., 3 months after ovariectomy (OVX vs. Sham: $p_{6M} = 0.0438$; $p_{7M} = 0.0209$).

To confirm the success of the ovariectomy, plasma LH concentrations were examined. A significant [age × group] interaction was found ($F_{2,37} = 31.63$; $p < 0.0001$; Fig. 1B), with significantly increased LH concentrations in the OVX group 1 month after the ovariectomy intervention ($p < 0.0001$ for all comparisons with 3 months), whereas no change was present in the Sham group. No difference in plasma LH was present at the baseline presurgery time point (OVX vs. Sham $p_{3M} > 0.99$); however, at every time point after ovariectomy intervention, LH concentrations were significantly higher in the OVX group than the Sham group ($p < 0.0001$ for all group comparisons after 3 months).

3.2. A-P brain FC is attenuated by ovariectomy

An initial analysis of the baseline rsfMRI data indicated no differences between 3-month-old mice, which were afterward randomly divided into the OVX or Sham group. Next, an ICA of the rsfMRI data at baseline conditions discerned several FC networks similar to previously described mouse rsfMRI networks (Supplementary Fig. S1) (Jonckers et al., 2011; Shah et al., 2016a; Zerbi et al., 2015). These included the functional anterior/prefrontal (Pf) and posterior/retrosplenial (Rs) networks, which were used for further A-P FC calculations (Fig. 2A), as it has been shown that these long-range connections are especially vulnerable to aging (Damoiseaux et al., 2008; Vidal-Pineiro et al., 2014). With reference to these networks, ROIs were defined to compute z-transformed FC matrices (Fig. 2B) from which FC between regions in the Pf and Rs network, i.e., A-P FC, was calculated (Fig. 2C).

Here, a significant group effect ($F_{4,32} = 4.93$; $p = 0.0337$) revealed that A-P FC in OVX mice was significantly lower than Sham mice. It can be appreciated from Fig. 2C that this effect was most pronounced at 7 months of age. A further hypothesis-driven analysis of potential group-specific aging effects revealed that only in the Sham group, a significant age-dependent strengthening of A-P FC could be observed (Sham: $F_{4,60} = 3.72$; $p = 0.0091$; OVX: $F_{4,61} = 0.70$; $p > 0.05$). More specifically, whereas A-P FC in OVX mice remained low and similar to baseline values throughout the study, Sham mice displayed an age-dependent strengthening of this connection when comparing baseline values at 3 months with A-P FC at the age of 6 (Sham 3M vs. 6M: $p = 0.0104$) and 7 months (Sham 3M vs. 7M: $p = 0.0164$). A linear regression analysis (Fig. 2D) further confirmed that a significant positive correlation between A-P FC and age was only present in Sham mice (Sham: $R^2 = 0.1369$, $p = 0.0007$; OVX: $R^2 = 0.006$, $p > 0.05$) and that this evolution differed significantly from the OVX group ($F_{1,154} = 6.057$, $p = 0.0150$).

Based on the FC pattern in Sham mice, two distinct age categories were identified: young adult between 3 and 5 months characterized by relatively low A-P FC, and adult between 6 and 7 months characterized by higher A-P FC. For each individual subject, the average FC was calculated for both age categories (Fig. 2D). By making this distinction, the observed effect was even more pronounced, with a significant [age × group] interaction effect ($F_{1,34} = 5.40$; $p = 0.0262$). Post hoc tests revealed that a significantly higher FC was present in adult sham mice, compared to adult OVX mice ($p = 0.0107$).

Next, a seed-based analysis of the left Rs region, i.e., the main seed for the posterior network, was performed to confirm the observed differences in A-P connectivity at the age of 7 months (Fig. 2E and F). From the individual FC maps, t-values and cluster size were extracted within the restrictions of the respective ICA component masks. Lower T-values were present in the anterior brain areas for 7-month-old OVX mice ($p = 0.0097$; Fig. 2F), indicating a reduced strength of FC between anterior regions and the Rs seed compared to age-matched sham mice. In addition, a smaller cluster size in both anterior and posterior regions ($p_{posterior} = 0.045$; $p_{anterior} = 0.011$) was present in the OVX mice, indicating a lower extent of FC with the Rs seed (Fig. 2F).

3.3. Cognitive impairments 4 months after ovariectomy

Based on the rsfMRI outcome, a set of behavioral tests tailored to assess the function of the Pf and Rs brain regions was selected to evaluate whether cognitive deficits were present alongside the FC alterations 4 months after ovariectomy. This selection of behavioral tests was further based on previous literature showing that performance in these tests can be modulated by hormonal alterations, as described previously in the respective Material and Methods section.

The PA test revealed a significant [test day × group] interaction effect ($F_{1,19} = 5.17$; $p = 0.0348$). *Post hoc* tests revealed that OVX mice did not present an increased latency to enter the dark compartment on the test day. In contrast, Sham mice had a significantly increased retention latency on the test day compared with the training day (Sham test day vs. Sham training day: $p = 0.0057$), and this latency was significantly longer than OVX mice at the test day (Test day Sham vs. OVX: $p = 0.0271$). These results indicate an impaired PA retention ability for the OVX group (Fig. 3A).

The Barnes maze test indicated that long-term spatial memory deficits were present in OVX mice (Fig. 2B–E). More specifically, OVX mice were able to learn the target spatial position as fast as Sham mice during training (data not shown). However, a marked smaller proportion of OVX mice presented a reduced retention ability during the single trial tests at 1 (day 5), 7 (day 12), and 14 days (day 19) after training. As such, only half of the OVX group successfully accomplishing this trial at day 19, 2 weeks after training (Fig. 3B). Compared with Sham mice, OVX mice made more primary errors ($F_{1,21} = 15.06$; $p = 0.0009$) with the most pronounced difference occurring on day 19 (Fig. 3C). Also, OVX mice had a consistently longer primary latency than Sham mice, indicating that they found their target hole slower ($F_{1,21} = 5.99$; $p = 0.0233$; Fig. 3D). Furthermore, OVX mice spent less time in the target zone than Sham mice ($F_{1,21} = 4.86$; $p = 0.0388$). It can be appreciated from Fig. 3E that this difference was most pronounced at day 19, i.e., 2 weeks after training.

The SA test, which assesses working memory dependent on hippocampal and frontal brain regions (Lalonde, 2002), did not reveal differences between both groups. Likewise, no differences were found for the NOR test that evaluates associative memory involving frontal and parietal association cortical regions (data not shown).

3.4. Molecular signaling alterations 4 months after ovariectomy

Based on the MRI outcome, Pf and Rs cortical samples were acquired from 7-month-old OVX and Sham mice to explore the underlying molecular signaling alterations. Using stringent and significant cutoff criteria for protein identification (99% percentile identification confidence) and significant deviation from the expression background (95% percentile deviation from control levels), we found that long-term HPG dysfunction, i.e., 4 months after ovariectomy, resulted in the significant alteration of multiple cortical proteins (Supplementary Fig. S2A): Pf cortex, 162 (140 upregulated, 22 downregulated; Supplementary Table S1) and Rs cortex, 230 (169 upregulated, 61 downregulated; Supplementary Table S2).

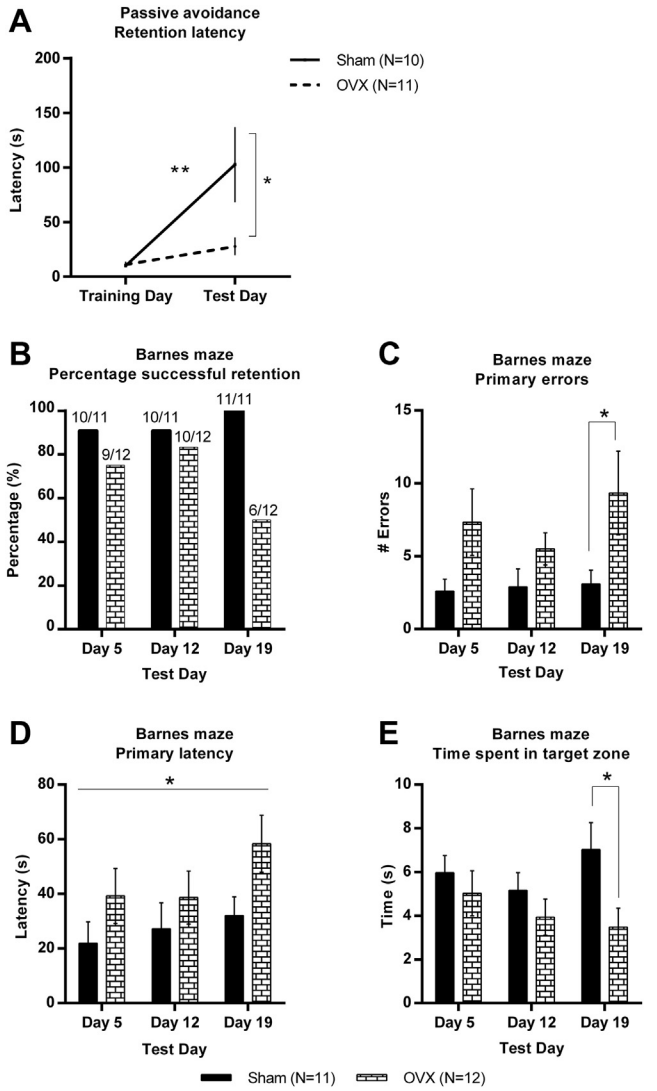

Fig. 3. Cognitive impairments after 4 months of endocrine disruption. (A) Retention latency for the passive avoidance (PA) test. Ovariectomized (OVX) mice did not display increased latency on the test day, reflecting impaired PA retention ability. (B-E) Barnes maze results. (B) Percentage of mice per group that reached the target hole on each test day—Numbers above the bars indicate the actual number of mice reaching the target hole compared to the total group size. Only half of the OVX mice were able to locate the target hole on day 19. (C) Number of primary errors on the test days—OVX mice made significantly more primary errors than Sham mice, especially on day 19. (D) Primary latency across the test days—OVX mice performed less well than the Sham mice ($p < 0.05$); however, no differences survived the multiple comparison correction. (E) Time spent in the target zone on each test day. OVX mice spent considerably less time in the target hole than the Sham group, an effect that was most pronounced on day 19. * $p < 0.05$; ** $p < 0.01$. Results are shown as mean ± SEM.

3.4.1. Canonical signaling pathway analysis

Quantitative proteomics is able to sample protein expression patterns at a mass level and is therefore able to, with effective bioinformatic interpretation, infer complex signaling behavior based on the co-expression of hundreds of proteins (Maudsley et al., 2011). Using these DEP profiles as inputs into IPA, we identified 17 and 15 significantly populated canonical signaling pathways, respectively (Supplementary Fig. S2B). Using a comparative hierarchical clustering of the significantly populated signaling pathways between the 2 cortex sources, we found that among the most highly enriched signaling pathways was the "*dopamine receptor signaling*" pathway (including proteins DAT or SLC6A3, dopamine transporter and DARPP32 or Ppp1r1b, Dopamine- and cAMP-regulated neuronal phosphoprotein). With respect to the distinctions between the two tissue sources, it was apparent that developmentally associated signaling pathways (e.g., "*TGF-beta signaling*," "*epithelial adherents junction signaling*," and "*osteoarthritis signaling*") were prominent in the Rs cortex, whereas pathways associated with neurotrophic and reproductive signaling (e.g., "*CREB signaling in neurons*," "*CDK5 signaling*," and "*relaxin signaling*") were prominent in the Pf samples.

3.4.2. Upstream functionality analysis

Next, we sought to identify potential protein/ligand-based factors whose perturbation may result in the generation of the DEP patterns we observed. These analyses in both cortical regions again predicted multiple dopamine-related factors that generate molecular signature alterations reminiscent of our DEP data sets from the 2 cortical samples (e.g., dopamine receptor D3 [DRD3] and nuclear receptor subfamily 4, group A, member 2 [NR4A2]; Montarolo et al., 2016; Reuter et al., 2017; Fig. 4A). We also found a clear distinction between the 2 regions with mainly altered neurodegenerative factors in the Rs cortex, while the Pf DEP patterns were more related to neurodevelopmental factors. A potential factor linking these 2 disparate events is likely to be the functionality of dopaminergic neural circuits that may facilitate this trans-cortex communication.

3.4.3. Western blot

Western blots were used to verify our findings. We first confirmed that ovariectomy intervention resulted in the significant upregulation of both rotatin (Rttn; $p = 0.0297$, n = 4) and syntaxin-4 (Stx4; $p = 0.0128$, n = 4) in the Pf cortex (Supplementary Fig. S2C). Next, we confirmed the significant downregulation of the relaxin-3 receptor (Rxfp3) in the Rs cortex after ovariectomy ($p = 0.0013$, n = 4; Supplementary Fig. S2D), supporting the bioinformatic analysis, which revealed a stronger representation of "relaxin signaling" in the Pf cortex as opposed to the Rs cortex (Supplementary Fig. S2B). It has been proposed that Rxfp3 receptor forms a close functional link (van Gastel et al., 2016) with the neurometabolic aging regulator, Git2 (G protein–coupled receptor kinase interacting protein 2; Chadwick et al., 2012; Lu et al., 2015; Martin et al., 2015; Siddiqui et al., 2017). With respect to this association, we found that alterations of cortical Git2 expression mirrored that of Rxfp3 (reduction in expression, $p = 0.0001$, n = 4), thus further reinforcing the posit that ovariectomy induces an accelerated aging phenotype as genomic deletion of Git2 is associated with accelerated aging and cellular senescence (Chadwick et al., 2012; Lu et al., 2015; Siddiqui et al., 2017).

3.4.4. Network-based deconvolution of the coherently regulated protein signatures

We next performed a more in-depth investigation into the interactive nature of the 31 proteins coherently regulated using a network topology-based approach. We identified 6 distinct functional subnetworks (SNs) of functionally associating proteins (Fig. 4B). The two largest SNs—SN1 and SN2—when investigated using GO term enrichment ($p < 0.05$, with >2 proteins per GO term group required for enrichment consideration) were both found to be associated with "*axogenesis*." Using a standard network graph annotation system (i.e., degree and betweenness "centrality"), SN1 was centered around *Nefl* (neurofilament light polypeptide), a protein strongly associated with "*neuronal structural regulation*," whereas SN2 was centered on the neuronal transmission-regulator *Mag* (myelin-associated glycoprotein). SNs 3 and 4 were associated with "*cell cycle activity*" (centered on *Sirt2*—NAD-dependent protein deacetylase sirtuin-2) and "*reproductive functionality*" (centered on *Cldn11*—Claudin 11), respectively. SNs 5 and 6 demonstrated a coherence of function as

SN5 was linked to "*neuronal transmission/apoptosis*" (centered on *Ache*—acetylcholinesterase), whereas SN6 was strongly linked to "*dopaminergic neurotransmission and secretion*" (centered on *Slc6a3*—sodium-dependent dopamine transporter).

3.4.5. Targeted NLP investigation of the DEP data sets

Finally, we identified the specific functional intersection between our own user-defined "*concept*" terms related to estrogenic activity in the brain and the DEP data sets from both cortical samples using a targeted NLP approach. As our experimental paradigm involved the direct implementation, via ovariectomy, of dramatic alterations in gonadal steroids, we next adopted an informatics approach to identify the specific functional intersection between steroid-related activity and our DEP data sets from both Pf and Rs cortex samples. For the 2 input DEP lists, the total cumulative cosine similarity scores for all the proteins demonstrating at least an implicit association (i.e., cosine similarity score > 0.1) with each of the denoted concept terms related to estrogenic activity in the brain are indicated in Fig. 4C. For each protein-term score combination, the number of proteins identified showing an implicit textual association with our user-defined concept (e.g., "menopause") is identified above the column. In addition, the highest cosine similarity–scoring protein from each sample against any of the specific concepts is indicated. For the majority, i.e., 4/5, both the number and degree of textual correlation to the specific concept were greater with the Rs than the Pf cortex data set DEPs. This perhaps suggests that the proteomic alterations here were most profoundly affected, compared with the Pf cortex samples, by disruption to estrogenic functionality. This also correlates to the more "pathological" alteration of signaling pathways and also reproductive signaling systems (e.g., the RXFP3 receptor) observed with our pathway analysis of Rs cortex samples compared with those from the PF cortex. Only the "*menopause*" input concept showed a greater association with the Pf cortex data.

Through ranking of the top 20 strongest correlating proteins, a prioritized key group of proteins for each DEP list was created. Using *Enrichr*-based interrogation of ligand-induced GEO data set alterations, we identified significantly overlapping GEO data set terms correlating to these top 20 DEPs. Extracting and then displaying, via word frequency-dependent wordclouds (font size indicating the relative frequencies), the words comprising these GEO perturbagen data sets a strong estrogen-related function was evident (Fig. 4D). When these 20 proteins were then cross-interrogated with a functional disease database, i.e., the JENSEN disease database (https://diseases.jensenlab.org/), a common signature of "*neurodegenerative disease*" was seen for Rs and Pf data sets. In agreement with our previous pathway analysis, the enrichment score (*Enrichr* "combined score") for the Rs cortex tissues was nearly twice that for the Pf cortex, reinforcing our hypothesis that an estrogen-mediated dysfunction induces a strong pro-neurodegenerative effect on the Rs cortex with a milder effect seen in the Pf cortex.

4. Discussion

Using the highly translational method of rsfMRI, we have demonstrated that endocrine disruption, by ovariectomy, prevented the strengthening of A-P connectivity between 3 and 7 months. In contrast to Sham mice, OVX mice displayed low A-P connectivity throughout the ages examined. The increase of this long-range FC in Sham mice likely reflects further maturation of the intrinsic functional networks, in line with data showing that although gross structural changes have already occurred by the age of 3 months in mice, minor alterations are still ongoing between 3 and 6 months of age (Hammelrath et al., 2016). Interestingly, long-range connections typically develop only later in life, toward adulthood (Dennis and Thompson, 2013; Fair et al., 2009), and have been previously identified to be more vulnerable to aging effects due to a complex interplay between structural and neurotransmission alterations as well as energy efficiency necessary to maintain these long-range connections (Tomasi and Volkow, 2012). As evidenced by our quantitative proteomics analysis, the FC pattern in OVX mice co-existed with an accelerated aging molecular phenotype (Fig. 3A–C). This is further supported by human studies (Levine et al., 2016; Rocca et al., 2016, 2017) showing that premature loss of gonadal hormones in women after bilateral ovariectomy is linked with signs of accelerated aging (Rocca et al., 2017).

We confirmed the co-existence of aberrant A-P FC and cognitive deficits in adult OVX mice, reflected by impaired memory retention in the Barnes maze and PA test. This is in agreement with human data showing that the strength of A-P FC is related to cognitive performance in healthy aging adults and patients with mild cognitive impairment (Liang et al., 2011; Vidal-Pineiro et al., 2014). As estrogen receptors are present in, among others, the hippocampus and cortical regions (Pf cortex) (Hazell et al., 2009; Mitra et al., 2003), these regions are highly targeted in OVX literature. In the present study, the earliest pathological signs were observed in cortical regions, i.e., the interaction between Pf and Rs regions, which is in agreement with the fact that we did not observe hippocampal-dependent learning deficits. In contrast to acquisition or memory formation, which involves hippocampal-cortical communication, memory retention is mainly driven by the integration of cortical regions (Bontempi et al., 1999; Izquierdo and Medina, 1997; Maviel et al., 2004; Miller, 2000; Todd and Bucci, 2015). In addition, the medial Pf cortex has been proposed to be involved in encoding fear learning (Herry and Johansen, 2014) corroborating the impaired PA performance demonstrated in OVX mice.

Although the Pf cortex is also important for functions such as working memory (Shanmugan and Epperson, 2014), we did not observe specific working memory deficits after ovariectomy, which is also supported by the fact that no local FC change was present in this region. In addition, working memory also relies on the integration of other brain areas, such as the hippocampus, perirhinal cortex, thalamus, and basal forebrain (Dere et al., 2007; Lalonde, 2002), so it is possible that these regions can compensate for any Pf dysfunction.

Although memory deficits in this study are in line with the posit that ovariectomy or menopause are linked with impaired cognitive function (Blair et al., 2016; Heikkinen et al., 2004; Iivonen et al., 2006), it is important to note that some discrepancies can be seen with respect to timing of ovariectomy and duration of hormone depletion as well as the variety in cognitive function investigated (Bastos et al., 2015; Heikkinen et al., 2004). One limitation within this study might be that we only evaluated behavioral performance at the age of 7 months, guided by the neuroimaging results. Therefore, no inference can be made as to which deficit occurred first: functional or behavioral impairments. Nevertheless, it is noteworthy that functional changes were only detectable 4 months after ovariectomy, which is coincident with the so-called "critical window" for estrogen replacement therapy (Blair et al., 2016). During this 4-month interval, many alterations might have occurred within the brain—as shown by our extensive proteomics analysis as well. As such, it can be argued that at this time point, the hormonal deprivation has led to irreversible changes to the neuronal system, including structural and neurotransmissive alterations. Therefore, FC alterations—and by extension also the behavioral changes—might also be driven by further downstream alterations in a cascade originally initiated by the ovariectomy intervention.

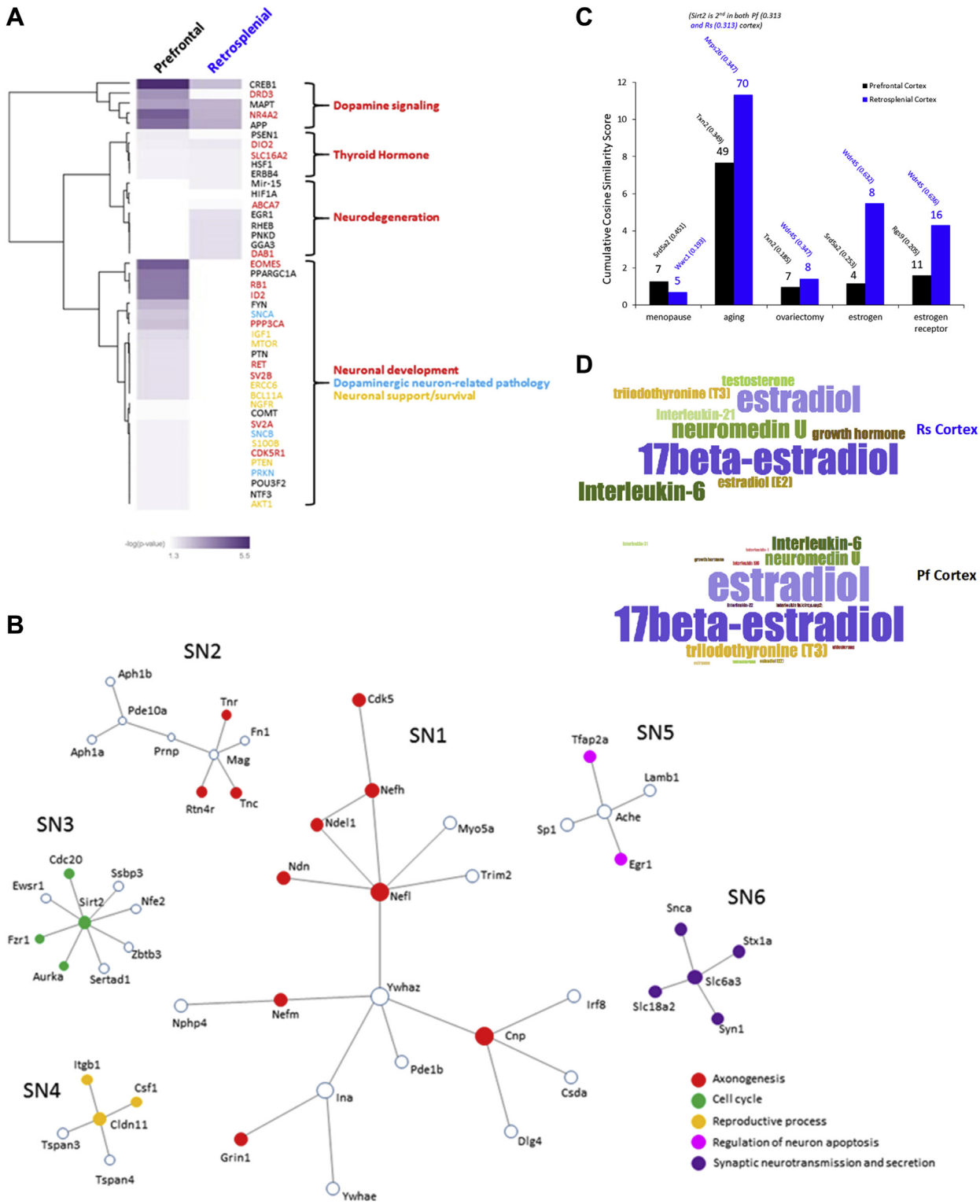

Fig. 4. Outcome of the quantitative proteomics. (A) IPA-based "upstream" functionality analysis. Regulators associated with dopamine-based signaling events were strongly linked to both cortex tissues while potential upstream regulators linked to neurodegeneration/thyroid hormone signaling were prominent in the retrosplenial cortex DEP patterns. DEP patterns from prefrontal cortical samples from OVX mice were under the influence of more complex signaling activity, involving potential regulators linked to neuronal development (red), generic neuronal support (yellow), or dopaminergic neuron pathology (turquoise). The associated key indicates the degree of pathway enrichment as a negative log10 of the primary probability value. (B) Network-based deconvolution of the coherently regulated protein signature common to prefrontal (Pf) and retrosplenial (Rs) cortex regions from OVX mice versus Sham mice. Six separate reliable SNs were found—termed SN1 to SN6. The two most complex networks (SN1 and SN2) were most strongly associated with axogenesis (proteins mediating this GO term enrichment are highlighted as red circles—a similar representation is made in the subsequent SNs), whereas SN3 and SN4 were associated with cell cycle activity (green circles) and reproductive process (orange circles), respectively. SNs 5 and 6 were both strongly associated with neurological functions, i.e., regulation of neuronal apoptosis (SN5, pink circles) or synaptic neurotransmission (SN6, purple circles). (C) Targeted natural language processing (NLP)—the graph shows the specific functional intersection between our user-defined "concept" terms related to estrogenic activity in the brain and the DEP data sets from both cortical samples. For each protein-term score combination, the number of proteins identified showing an implicit textual association with our user-defined concept is identified above the column. In addition,

Further investigation into the molecular signaling pattern underlying FC and cognitive changes indicated alterations of multiple proteins reflecting a neurodegenerative or neurodevelopmental pathology in the Rs and Pf cortices, respectively. The upregulation of prodevelopmental and neuronal survival factors within the Pf region could be explained by the high level of resilience and neuroplasticity in this region throughout life (Kolb and Gibb, 2015). Reinforcement of these processes also supports the idea that OVX mice might demonstrate a compensatory mechanism to preserve the local FC and prevent further deterioration. Nevertheless, despite these seemingly positive reinforcement mechanisms, the DEP patterns from the Pf region were also strongly related with estrogenic dysfunction, aging, and neurodegeneration. Although molecular alterations in both regions were clearly linked to hormonal and neurodegenerative processes, as shown by the NLP analysis, it was obvious that the Rs cortex was most affected both by number and degree of textual correlation to our specific "*concept*" terms. This perhaps suggests that the proteomic alterations here were most profoundly affected, compared to the Pf cortex samples, by disruption to estrogenic functionality. This also correlates to the more "pathological" alteration of signaling pathways and also reproductive signaling systems (e.g., the RXFP3 receptor) observed with our pathway analysis of Rs cortex samples compared with those from the Pf cortex. Only the "menopause" input concept showed a greater association with the Pf cortex data. It is interesting to note that here we found an alteration in the expression of Srd5a2 (3-oxo-5α-steroid 4-dehydrogenase 2, or 5-alpha reductase 2). This enzyme is involved in the functional processing of androgens, and thus its elevation in the Pf cortex region may be indicative of an ameliorative response in this brain region to compensate the more pathological signatures observed in the Rs cortex.

Although a clear distinct pattern was present in both regions, we also found a considerable proportion of commonality between both regions. On the protein-level, both regions showed a significant upregulation of Rttn. This protein is implicated in early cortical development, and mutations of the Rttn gene can lead to microcephaly and polymicrogyria (Kheradmand Kia et al., 2012; Shamseldin et al., 2015). However, it has never been described before in the adult brain. It is possible that after the ovariectomy intervention, neurons are forced to take on a more immature state due to the loss of normal hormonal input signaling, which might explain increased expression of such developmental protein. Further research is required to unravel its role in the adult brain and its implication in the hormonal regulation of brain structure and function.

According to the network-based deconvolution of the common DEP list, the axogenesis SN was centered on Nefl, an important neural cytoskeleton protein. An increase of Nefl has been previously linked to axonal damage and has thus been proposed as a promising marker for the progression of neurodegenerative disorders (Bacioglu et al., 2016). Besides these structural alterations, the driving force behind the observed FC and cognitive deficits was most likely altered dopaminergic function as this was found to be most significantly altered in both regions in the pathway and upstream regulator analyses. The link between the dopaminergic system, cognition, and hormones is supported by several studies (Barth et al., 2015; Bosse and DiPaolo, 1996; Izquierdo and Medina, 1997; Jacobs and D'Esposito, 2011). Here, we found reduced FC coincident with upregulation of dopamine-related proteins after ovariectomy. Indeed, it has been proposed that both insufficient and excessive levels of dopamine can lead to Pf dysfunction and cognitive deficits (Jacobs and D'Esposito, 2011). Furthermore, a predicted common upstream regulator found in both regions was DRD3, which is implicated in synaptic plasticity and memory processes. This is in line with data showing that DRD3-knockout mice present improved cognitive function both after ovariectomy (Cao et al., 2013) and on aging (Xing et al., 2010). Moreover, antagonists for DRD3 have been proposed to benefit cognitive function and learning performance in rodents (Laszy et al., 2005). It is further interesting to note that for the Pf sample disease analysis, a nerve conduction disorder was prominent in the output data, i.e., "Canavan disease" [DOID:3613: https://diseases.jensenlab.org/]. This finding indicates that potential dysmyelination of the dopaminergic tracts between the Pf and Rs cortices may underpin the neurodegenerative effect induced by HPG dysfunction.

Finally, it is important to mention that the scope of our present study was to first examine whether resting-state functional alterations occur after endocrine disruptions and, secondly, to evaluate the ability of neuroimage-guided molecular investigations to elucidate and help interpret complex molecular phenotypes. In this present study, however, we cannot discount that the endocrine disruptions observed, and not potential epigenetic, metabolic, or vascular alterations, are solely the cause of the DEP patterns observed in the 2 differing brain regions. These questions, however, remain an important potential new avenue for our continued research.

5. Conclusion

Within the present study, we have shown that ovariectomy in mice attenuates long-range A-P FC and leads to cognitive deficits at adult age. We identified that these functional and cognitive changes were driven by underlying pathological molecular signaling patterns, reflecting an imbalance between pro-neurodevelopmental and pro-neurodegenerative processes in the Pf and Rs cortices, respectively. The molecular phenotype further showed a strong involvement of changes in aging and reproductive signaling, as well as altered structural aspects (axogenesis, myelination) and dopaminergic neurotransmissive function. These findings support the proposed detrimental impact of endocrine disruption on brain function and cognition as well as the potential of using resting-state FC as a translational noninvasive readout.

Disclosure

The authors report no actual or potential conflict of interest.

Acknowledgements

The authors thank Jonathan Janssens (Translational Neurobiology Group, University of Antwerp-VIB) and Charlotte Vanacker (Inserm U1172, University of Lille) for their technical assistance. This research was supported by the European Union's Seventh Framework Program under grant agreement number 278850 (INMiND), the Fund for Scientific Research Flanders (FWO) (grant agreements G057615N and 12S4815N), the Stichting Alzheimer Onderzoek (SAO-FRA, grant agreement 13026), the interdisciplinary PhD grant BOF DOCPRO 2014 (granted to MV), by a KP-BOF 2015 from the University of Antwerp (granted to FK) and by the

the highest cosine similarity—scoring protein from each sample against any of the specific concepts is indicated. (D) Wordclouds showing a strong relation between our DEP profiles and estrogenic function. The significant overlap between the top 20 strongest correlating proteins (based on C) and GEO perturbagen data sets is presented as a word frequency—dependent wordcloud (font size indicating the relative frequencies). Abbreviations: IPA, Ingenuity Pathway Analysis; DEP, differentially expressed protein; GEO, Gene Expression Omnibus; OVX, ovariectomized; SN, subnetworks. (For interpretation of the references to color in this figure legend, the reader is referred to the Web version of this article.)

Agence Nationale de la Recherche (ANR GRAND, ANR-17-CE16-0015-01 to VP). The authors thank the behavioral exploration platform for rodents (Federation of Neurosciences, Univ Lille, France) and Dr Charlotte Laloux for her advices on behavioral analysis. The 9.4T Bruker MR system was in part funded by the Flemish Impulse funding for heavy scientific equipment (42/FA010100/123) granted to Prof. Dr Annemie Van der Linden.

Appendix A. Supplementary data

Supplementary data to this article can be found online at https://doi.org/10.1016/j.neurobiolaging.2018.10.012.

References

Albertson, A.J., Navratil, A., Mignot, M., Dufourny, L., Cherrington, B., Skinner, D.C., 2008. Immunoreactive GnRH type I receptors in the mouse and sheep brain. J. Chem. Neuroanat. 35, 326–333.
Andrews-Hanna, J.R., Snyder, A.Z., Vincent, J.L., Lustig, C., Head, D., Raichle, M.E., Buckner, R.L., 2007. Disruption of large-scale brain systems in advanced aging. Neuron 56, 924–935.
Arevalo, M.A., Azcoitia, I., Garcia-Segura, L.M., 2015. The neuroprotective actions of oestradiol and oestrogen receptors. Nat. Rev. Neurosci. 16, 17–29.
Bacioglu, M., Maia, L.F., Preische, O., Schelle, J., Apel, A., Kaeser, S.A., Schweighauser, M., Eninger, T., Lambert, M., Pilotto, A., Shimshek, D.R., Neumann, U., Kahle, P.J., Staufenbiel, M., Neumann, M., Maetzler, W., Kuhle, J., Jucker, M., 2016. Neurofilament light chain in blood and CSF as marker of disease progression in mouse models and in neurodegenerative diseases. Neuron 91, 494–496.
Barth, C., Villringer, A., Sacher, J., 2015. Sex hormones affect neurotransmitters and shape the adult female brain during hormonal transition periods. Front. Neurosci. 9, 37.
Bastos, C.P., Pereira, L.M., Ferreira-Vieira, T.H., Drumond, L.E., Massensini, A.R., Moraes, M.F., Pereira, G.S., 2015. Object recognition memory deficit and depressive-like behavior caused by chronic ovariectomy can be transitorialy recovered by the acute activation of hippocampal estrogen receptors. Psychoneuroendocrinology 57, 14–25.
Blair, J.A., McGee, H., Bhatta, S., Palm, R., Casadesus, G., 2015. Hypothalamic-pituitary-gonadal axis involvement in learning and memory and Alzheimer's disease: more than "just" estrogen. Front. Endocrinol. (Lausanne) 6, 45.
Blair, J.A., Palm, R., Chang, J., McGee, H., Zhu, X., Wang, X., Casadesus, G., 2016. Luteinizing hormone downregulation but not estrogen replacement improves ovariectomy-associated cognition and spine density loss independently of treatment onset timing. Horm. Behav. 78, 60–66.
Bontempi, B., Laurent-Demir, C., Destrade, C., Jaffard, R., 1999. Time-dependent reorganization of brain circuitry underlying long-term memory storage. Nature 400, 671–675.
Bosse, R., DiPaolo, T., 1996. The modulation of brain dopamine and GABAA receptors by estradiol: a clue for CNS changes occurring at menopause. Cell Mol. Neurobiol. 16, 199–212.
Brann, D.W., Dhandapani, K., Wakade, C., Mahesh, V.B., Khan, M.M., 2007. Neurotrophic and neuroprotective actions of estrogen: basic mechanisms and clinical implications. Steroids 72, 381–405.
Cai, H., Chen, H., Yi, T., Daimon, C.M., Boyle, J.P., Peers, C., Maudsley, S., Martin, B., 2013. VennPlex–a novel Venn diagram program for comparing and visualizing datasets with differentially regulated datapoints. PLoS One 8, e53388.
Cao, F., Zhang, H., Meng, X., Feng, J., Li, T., Wei, S., Li, S., 2013. Ovariectomy-mediated impairment of spatial working memory, but not reference memory, is attenuated by the knockout of the dopamine D(3) receptor in female mice. Behav. Brain Res. 247, 27–33.
Cashion, A., Stanfill, A., Thomas, F., Xu, L., Sutter, T., Eason, J., Ensell, M., Homayouni, R., 2013. Expression levels of obesity-related genes are associated with weight change in kidney transplant recipients. PLoS One 8, e59962.
Chadwick, W., Martin, B., Chapter, M.C., Park, S.S., Wang, L., Daimon, C.M., Brenneman, R., Maudsley, S., 2012. GIT2 acts as a potential keystone protein in functional hypothalamic networks associated with age-related phenotypic changes in rats. PLoS One 7, e36975.
Chen, H., Martin, B., Daimon, C.M., Maudsley, S., 2013. Effective use of latent semantic indexing and computational linguistics in biological and biomedical applications. Front. Physiol. 4, 8.
Comasco, E., Sundstrom-Poromaa, I., 2015. Neuroimaging the menstrual cycle and premenstrual dysphoric disorder. Curr. Psychiatry Rep. 17, 77.
Damoiseaux, J.S., Beckmann, C.F., Arigita, E.J., Barkhof, F., Scheltens, P., Stam, C.J., Smith, S.M., Rombouts, S.A., 2008. Reduced resting-state brain activity in the "default network" in normal aging. Cereb. Cortex 18, 1856–1864.
Das, A., Dikshit, M., Srivastava, S.R., Srivastava, U.K., Nath, C., 2002. Effect of ovariectomy and estrogen supplementation on brain acetylcholinesterase activity and passive-avoidance learning in rats. Can. J. Physiol. Pharmacol. 80, 907–914.
De Bondt, T., Smeets, D., Pullens, P., Van Hecke, W., Jacquemyn, Y., Parizel, P.M., 2015. Stability of resting state networks in the female brain during hormonal changes and their relation to premenstrual symptoms. Brain Res. 1624, 275–285.
Dennis, E.L., Thompson, P.M., 2013. Typical and atypical brain development: a review of neuroimaging studies. Dialogues Clin. Neurosci. 15, 359–384.
Dere, E., Huston, J.P., De Souza Silva, M.A., 2007. The pharmacology, neuroanatomy and neurogenetics of one-trial object recognition in rodents. Neurosci. Biobehav. Rev. 31, 673–704.
Fair, D.A., Cohen, A.L., Power, J.D., Dosenbach, N.U., Church, J.A., Miezin, F.M., Schlaggar, B.L., Petersen, S.E., 2009. Functional brain networks develop from a "local to distributed" organization. PLoS Comput. Biol. 5, e1000381.
Fonseca, C.S., Gusmao, I.D., Raslan, A.C., Monteiro, B.M., Massensini, A.R., Moraes, M.F., Pereira, G.S., 2013. Object recognition memory and temporal lobe activation after delayed estrogen replacement therapy. Neurobiol. Learn. Mem. 101, 19–25.
Franklin, K.B.J., Paxinos, G., 2007. The Mouse Brain in Stereotaxic Coordinates, 3 ed. Elsevier, Amsterdam.
Hammelrath, L., Skokic, S., Khmelinskii, A., Hess, A., van der Knaap, N., Staring, M., Lelieveldt, B.P.F., Wiedermann, D., Hoehn, M., 2016. Morphological maturation of the mouse brain: an in vivo MRI and histology investigation. Neuroimage 125, 144–152.
Hara, Y., Waters, E.M., McEwen, B.S., Morrison, J.H., 2015. Estrogen effects on cognitive and synaptic health over the lifecourse. Physiol. Rev. 95, 785–807.
Hazell, G.G., Yao, S.T., Roper, J.A., Prossnitz, E.R., O'Carroll, A.M., Lolait, S.J., 2009. Localisation of GPR30, a novel G protein-coupled oestrogen receptor, suggests multiple functions in rodent brain and peripheral tissues. J. Endocrinol. 202, 223–236.
Heikkinen, T., Puolivali, J., Tanila, H., 2004. Effects of long-term ovariectomy and estrogen treatment on maze learning in aged mice. Exp. Gerontol. 39, 1277–1283.
Henderson, V.W., 2014. Alzheimer's disease: review of hormone therapy trials and implications for treatment and prevention after menopause. J. Steroid Biochem. Mol. Biol. 142, 99–106.
Herry, C., Johansen, J.P., 2014. Encoding of fear learning and memory in distributed neuronal circuits. Nat. Neurosci. 17, 1644–1654.
Hjelmervik, H., Hausmann, M., Osnes, B., Westerhausen, R., Specht, K., 2014. Resting states are resting traits–an FMRI study of sex differences and menstrual cycle effects in resting state cognitive control networks. PLoS One 9, e103492.
Horstink, M.W., Strijks, E., Dluzen, D.E., 2003. Estrogen and Parkinson's disease. Adv. Neurol. 91, 107–114.
Huang, J., Bai, F., Yang, X., Chen, C., Bao, X., Zhang, Y., 2015. Identifying brain functional alterations in postmenopausal women with cognitive impairment. Maturitas 81, 371–376.
Hughes, R.N., 2004. The value of spontaneous alternation behavior (SAB) as a test of retention in pharmacological investigations of memory. Neurosci. Biobehav. Rev. 28, 497–505.
Iivonen, S., Heikkinen, T., Puolivali, J., Helisalmi, S., Hiltunen, M., Soininen, H., Tanila, H., 2006. Effects of estradiol on spatial learning, hippocampal cytochrome P450 19, and estrogen alpha and beta mRNA levels in ovariectomized female mice. Neuroscience 137, 1143–1152.
Izquierdo, I., Medina, J.H., 1997. Memory formation: the sequence of biochemical events in the hippocampus and its connection to activity in other brain structures. Neurobiol. Learn Mem. 68, 285–316.
Jacobs, E., D'Esposito, M., 2011. Estrogen shapes dopamine-dependent cognitive processes: implications for women's health. J. Neurosci. 31, 5286–5293.
Jonckers, E., Van Audekerke, J., De Visscher, G., Van der Linden, A., Verhoye, M., 2011. Functional connectivity fMRI of the rodent brain: comparison of functional connectivity networks in rat and mouse. PLoS One 6, e18876.
Kheradmand Kia, S., Verbeek, E., Engelen, E., Schot, R., Poot, R.A., de Coo, I.F., Lequin, M.H., Poulton, C.J., Pourfarzad, F., Grosveld, F.G., Brehm, A., de Wit, M.C., Oegema, R., Dobyns, W.B., Verheijen, F.W., Mancini, G.M., 2012. RTTN mutations link primary cilia function to organization of the human cerebral cortex. Am. J. Hum. Genet. 91, 533–540.
Koebele, S.V., Bimonte-Nelson, H.A., 2016. Modeling menopause: the utility of rodents in translational behavioral endocrinology research. Maturitas 87, 5–17.
Koebele, S.V., Bimonte-Nelson, H.A., 2017. The endocrine-brain-aging triad where many paths meet: female reproductive hormone changes at midlife and their influence on circuits important for learning and memory. Exp. Gerontol. 94, 14–23.
Kolb, B., Gibb, R., 2015. Plasticity in the prefrontal cortex of adult rats. Front. Cell Neurosci. 9, 15.
Lalonde, R., 2002. The neurobiological basis of spontaneous alternation. Neurosci. Biobehav. Rev. 26, 91–104.
Langbeen, A., Ginneken, C.V., Fransen, E., Bosmans, E., Leroy, J., Bols, P.E.J., 2016. Morphometrical analysis of preantral follicular survival of VEGF-treated bovine ovarian cortex tissue following xenotransplantation in an immune deficient mouse model. Anim. Reprod. Sci. 168, 73–85.
Laszy, J., Laszlovszky, I., Gyertyan, I., 2005. Dopamine D3 receptor antagonists improve the learning performance in memory-impaired rats. Psychopharmacology (Berl) 179, 567–575.
Leger, M., Quiedeville, A., Bouet, V., Haelewyn, B., Boulouard, M., Schumann-Bard, P., Freret, T., 2013. Object recognition test in mice. Nat. Protoc. 8, 2531–2537.
Levine, M.E., Lu, A.T., Chen, B.H., Hernandez, D.G., Singleton, A.B., Ferrucci, L., Bandinelli, S., Salfati, E., Manson, J.E., Quach, A., Kusters, C.D., Kuh, D., Wong, A., Teschendorff, A.E., Widschwendter, M., Ritz, B.R., Absher, D., Assimes, T.L., Horvath, S., 2016. Menopause accelerates biological aging. Proc. Natl. Acad. Sci. U. S. A. 113, 9327–9332.
Li, R., Cui, J., Shen, Y., 2014. Brain sex matters: estrogen in cognition and Alzheimer's disease. Mol. Cell Endocrinol. 389, 13–21.

Liang, P., Wang, Z., Yang, Y., Jia, X., Li, K., 2011. Functional disconnection and compensation in mild cognitive impairment: evidence from DLPFC connectivity using resting-state fMRI. PLoS One 6, e22153.
Lisofsky, N., Martensson, J., Eckert, A., Lindenberger, U., Gallinat, J., Kuhn, S., 2015. Hippocampal volume and functional connectivity changes during the female menstrual cycle. Neuroimage 118, 154–162.
Lu, D., Cai, H., Park, S.S., Siddiqui, S., Premont, R.T., Schmalzigaug, R., Paramasivam, M., Seidman, M., Bodogai, I., Biragyn, A., Daimon, C.M., Martin, B., Maudsley, S., 2015. Nuclear GIT2 is an ATM substrate and promotes DNA repair. Mol. Cell Biol. 35, 1081–1096.
Marciniak, E., Faivre, E., Dutar, P., Alves Pires, C., Demeyer, D., Caillierez, R., Laloux, C., Buee, L., Blum, D., Humez, S., 2015. The Chemokine MIP-1alpha/CCL3 impairs mouse hippocampal synaptic transmission, plasticity and memory. Sci. Rep. 5, 15862.
Martin, B., Chadwick, W., Janssens, J., Premont, R.T., Schmalzigaug, R., Becker, K.G., Lehrmann, E., Wood, W.H., Zhang, Y., Siddiqui, S., Park, S.S., Cong, W.N., Daimon, C.M., Maudsley, S., 2015. GIT2 acts as a systems-level coordinator of neurometabolic activity and pathophysiological aging. Front. Endocrinol. (Lausanne) 6, 191.
Maudsley, S., Chadwick, W., Wang, L., Zhou, Y., Martin, B., Park, S.S., 2011. Bioinformatic approaches to metabolic pathways analysis. Methods Mol. Biol. 756, 99–130.
Maviel, T., Durkin, T.P., Menzaghi, F., Bontempi, B., 2004. Sites of neocortical reorganization critical for remote spatial memory. Science 305, 96–99.
Messina, A., Langlet, F., Chachlaki, K., Roa, J., Rasika, S., Jouy, N., Gallet, S., Gaytan, F., Parkash, J., Tena-Sempere, M., Giacobini, P., Prevot, V., 2016. A microRNA switch regulates the rise in hypothalamic GnRH production before puberty. Nat. Neurosci. 19, 835–844.
Miller, E.K., 2000. The prefrontal cortex and cognitive control. Nat. Rev. Neurosci. 1, 59–65.
Mitra, S.W., Hoskin, E., Yudkovitz, J., Pear, L., Wilkinson, H.A., Hayashi, S., Pfaff, D.W., Ogawa, S., Rohrer, S.P., Schaeffer, J.M., McEwen, B.S., Alves, S.E., 2003. Immunolocalization of estrogen receptor beta in the mouse brain: comparison with estrogen receptor alpha. Endocrinology 144, 2055–2067.
Montarolo, F., Perga, S., Martire, S., Navone, D.N., Marchet, A., Leotta, D., Bertolotto, A., 2016. Altered NR4A subfamily gene expression level in peripheral blood of Parkinson's and Alzheimer's disease patients. Neurotox Res. 30, 338–344.
Parker, W.H., Jacoby, V., Shoupe, D., Rocca, W., 2009. Effect of bilateral oophorectomy on women's long-term health. Womens Health (Lond) 5, 565–576.
Peper, J.S., van den Heuvel, M.P., Mandl, R.C., Hulshoff Pol, H.E., van Honk, J., 2011. Sex steroids and connectivity in the human brain: a review of neuroimaging studies. Psychoneuroendocrinology 36, 1101–1113.
Ping, S.E., Trieu, J., Wlodek, M.E., Barrett, G.L., 2008. Effects of estrogen on basal forebrain cholinergic neurons and spatial learning. J. Neurosci. Res. 86, 1588–1598.
Reuter, M.S., Krumbiegel, M., Schluter, G., Ekici, A.B., Reis, A., Zweier, C., 2017. Haploinsufficiency of NR4A2 is associated with a neurodevelopmental phenotype with prominent language impairment. Am. J. Med. Genet. A. 173, 2231–2234.
Rocca, W.A., Bower, J.H., Maraganore, D.M., Ahlskog, J.E., Grossardt, B.R., de Andrade, M., Melton 3rd, L.J., 2008a. Increased risk of parkinsonism in women who underwent oophorectomy before menopause. Neurology 70, 200–209.
Rocca, W.A., Gazzuola-Rocca, L., Smith, C.Y., Grossardt, B.R., Faubion, S.S., Shuster, L.T., Kirkland, J.L., Stewart, E.A., Miller, V.M., 2016. Accelerated Accumulation of Multimorbidity after bilateral oophorectomy: a population-based cohort study. Mayo Clin. Proc. 91, 1577–1589.
Rocca, W.A., Gazzuola Rocca, L., Smith, C.Y., Grossardt, B.R., Faubion, S.S., Shuster, L.T., Kirkland, J.L., Stewart, E.A., Miller, V.M., 2017. Bilateral oophorectomy and accelerated aging: cause or effect? J. Gerontol. A. Biol. Sci. Med. Sci. 72, 1213–1217.
Rocca, W.A., Grossardt, B.R., Geda, Y.E., Gostout, B.S., Bower, J.H., Maraganore, D.M., de Andrade, M., Melton 3rd, L.J., 2008b. Long-term risk of depressive and anxiety symptoms after early bilateral oophorectomy. Menopause 15, 1050–1059.
Rocca, W.A., Grossardt, B.R., Shuster, L.T., 2011. Oophorectomy, menopause, estrogen treatment, and cognitive aging: clinical evidence for a window of opportunity. Brain Res. 1379, 188–198.
Ryan, K.D., Schwartz, N.B., 1980. Changes in serum hormone levels associated with male-induced ovulation in group-housed adult female mice. Endocrinology 106, 959–966.
Sacher, J., Okon-Singer, H., Villringer, A., 2013. Evidence from neuroimaging for the role of the menstrual cycle in the interplay of emotion and cognition. Front. Hum. Neurosci. 7, 374.
Sakaki, M., Mather, M., 2012. How reward and emotional stimuli induce different reactions across the menstrual cycle. Soc. Personal. Psychol. Compass 6, 1–17.
Sandstrom, N.J., Williams, C.L., 2001. Memory retention is modulated by acute estradiol and progesterone replacement. Behav. Neurosci. 115, 384–393.
Sarkaki, A., Amani, R., Badavi, M., Safahani, M., Aligholi, H., 2008. Effect of ovariectomy on reference memory version of Morris water maze in young adult rats. Iran Biomed. J. 12, 123–128.
Shah, D., Blockx, I., Keliris, G.A., Kara, F., Jonckers, E., Verhoye, M., Van der Linden, A., 2016a. Cholinergic and serotonergic modulations differentially affect large-scale functional networks in the mouse brain. Brain Struct. Funct. 221, 3067–3079.
Shah, D., Deleye, S., Verhoye, M., Staelens, S., Van der Linden, A., 2016b. Resting-state functional MRI and [18F]-FDG PET demonstrate differences in neuronal activity between commonly used mouse strains. Neuroimage 125, 571–577.
Shah, D., Latif-Hernandez, A., De Strooper, B., Saito, T., Saido, T., Verhoye, M., D'Hooge, R., Van der Linden, A., 2018. Spatial reversal learning defect coincides with hypersynchronous telencephalic BOLD functional connectivity in APP(NL-F/NL-F) knock-in mice. Sci. Rep. 8, 6264.
Shah, D., Praet, J., Latif Hernandez, A., Hofling, C., Anckaerts, C., Bard, F., Morawski, M., Detrez, J.R., Prinsen, E., Villa, A., De Vos, W.H., Maggi, A., D'Hooge, R., Balschun, D., Rossner, S., Verhoye, M., Van der Linden, A., 2016c. Early pathologic amyloid induces hypersynchrony of BOLD resting-state networks in transgenic mice and provides an early therapeutic window before amyloid plaque deposition. Alzheimers Dement. 12, 964–976.
Shamseldin, H., Alazami, A.M., Manning, M., Hashem, A., Caluseiu, O., Tabarki, B., Esplin, E., Schelley, S., Innes, A.M., Parboosingh, J.S., Lamont, R., Care4Rare Canada, C., Majewski, J., Bernier, F.P., Alkuraya, F.S., 2015. RTTN mutations cause primary microcephaly and primordial dwarfism in humans. Am. J. Hum. Genet. 97, 862–868.
Shanmugan, S., Epperson, C.N., 2014. Estrogen and the prefrontal cortex: towards a new understanding of estrogen's effects on executive functions in the menopause transition. Hum. Brain Mapp. 35, 847–865.
Shughrue, P.J., Lane, M.V., Merchenthaler, I., 1997. Comparative distribution of estrogen receptor-alpha and -beta mRNA in the rat central nervous system. J. Comp. Neurol. 388, 507–525.
Siddiqui, S., Lustig, A., Carter, A., Sankar, M., Daimon, C.M., Premont, R.T., Etienne, H., van Gastel, J., Azmi, A., Janssens, J., Becker, K.G., Zhang, Y., Wood, W., Lehrmann, E., Martin, J.G., Martin, B., Taub, D.D., Maudsley, S., 2017. Genomic deletion of GIT2 induces a premature age-related thymic dysfunction and systemic immune system disruption. Aging (Albany, NY) 9, 706–740.
Steyn, F.J., Wan, Y., Clarkson, J., Veldhuis, J.D., Herbison, A.E., Chen, C., 2013. Development of a methodology for and assessment of pulsatile luteinizing hormone secretion in juvenile and adult male mice. Endocrinology 154, 4939–4945.
Sundstrom Poromaa, I., Gingnell, M., 2014. Menstrual cycle influence on cognitive function and emotion processing-from a reproductive perspective. Front. Neurosci. 8, 380.
Sunyer, B., Patil, S., Höger, H., Lubec, G., 2007. Barnes Maze, a Useful Task to Assess Spatial Reference Memory in the Mice. Nature Publishing Group, Protocol Exchange. https://doi.org/10.1038/nprot.2007.390.
Todd, T.P., Bucci, D.J., 2015. Retrosplenial cortex and long-term memory: Molecules to behavior. Neural plasticity 2015, 414173.
Toffoletto, S., Lanzenberger, R., Gingnell, M., Sundstrom-Poromaa, I., Comasco, E., 2014. Emotional and cognitive functional imaging of estrogen and progesterone effects in the female human brain: a systematic review. Psychoneuroendocrinology 50, 28–52.
Tomasi, D., Volkow, N.D., 2012. Aging and functional brain networks. Mol. Psychiatry 17, 471, 549-458.
van den Heuvel, M.P., Hulshoff Pol, H.E., 2010. Exploring the brain network: a review on resting-state fMRI functional connectivity. Eur. Neuropsychopharmacol. 20, 519–534.
van Gastel, J., Janssens, J., Etienne, H., Azmi, A., Maudsley, S., 2016. The synergistic GIT2-RXFP3 system in the brain and its importance in age-related disorders. Front. Aging Neurosci. https://doi.org/10.3389/conf.fnagi.2016.03.00042.
Vargas, K.G., Milic, J., Zaciragic, A., Wen, K.X., Jaspers, L., Nano, J., Dhana, K., Bramer, W.M., Kraja, B., van Beeck, E., Ikram, M.A., Muka, T., Franco, O.H., 2016. The functions of estrogen receptor beta in the female brain: a systematic review. Maturitas 93, 41–57.
Vega, J.N., Zurkovsky, L., Albert, K., Melo, A., Boyd, B., Dumas, J., Woodward, N., McDonald, B.C., Saykin, A.J., Park, J.H., Naylor, M., Newhouse, P.A., 2016. Altered brain connectivity in early postmenopausal women with subjective cognitive impairment. Front. Neurosci. 10, 433.
Vidal-Pineiro, D., Valls-Pedret, C., Fernandez-Cabello, S., Arenaza-Urquijo, E.M., Sala-Llonch, R., Solana, E., Bargallo, N., Junque, C., Ros, E., Bartres-Faz, D., 2014. Decreased Default Mode Network connectivity correlates with age-associated structural and cognitive changes. Front. Aging Neurosci. 6, 256.
Vina, J., Lloret, A., 2010. Why women have more Alzheimer's disease than men: gender and mitochondrial toxicity of amyloid-beta peptide. J. Alzheimers Dis. 20 (Suppl 2), S527–S533.
Wang, L., Chadwick, W., Park, S.S., Zhou, Y., Silver, N., Martin, B., Maudsley, S., 2010. Gonadotropin-releasing hormone receptor system: modulatory role in aging and neurodegeneration. CNS Neurol. Disord. Drug Targets 9, 651–660.
Wen, S., Gotze, I.N., Mai, O., Schauer, C., Leinders-Zufall, T., Boehm, U., 2011. Genetic identification of GnRH receptor neurons: a new model for studying neural circuits underlying reproductive physiology in the mouse brain. Endocrinology 152, 1515–1526.
Whitten, W.K., 1956. Modification of the oestrous cycle of the mouse by external stimuli associated with the male. J. Endocrinol. 13, 399–404.
Xing, B., Meng, X., Wei, S., Li, S., 2010. Influence of dopamine D3 receptor knockout on age-related decline of spatial memory. Neurosci. Lett. 481, 149–153.
Zarate, S., Stevnsner, T., Gredilla, R., 2017. Role of estrogen and other sex hormones in brain aging. Neuroprotection and DNA repair. Front. Aging Neurosci. 9, 430.
Zerbi, V., Grandjean, J., Rudin, M., Wenderoth, N., 2015. Mapping the mouse brain with rs-fMRI: an optimized pipeline for functional network identification. Neuroimage 123, 11–21.